ORIGINAL ARTICLE

Synthesis of taurine–fluorescein conjugate and evaluation of its retina-targeted efficiency *in vitro*

CrossMark

Meihong Huang[a,b], Jiaqi Song[a], Bingzheng Lu[c], Huizhi Huang[a], Yizhen Chen[a], Wei Yin[c], Wenbo Zhu[c], Xinwen Su[c], Chuanbin Wu[a], Haiyan Hu[a,*]

[a]*Laboratory of Pharmaceutics, School of Pharmaceutical Sciences, Sun Yat-sen University, Guangzhou 510006, China*
[b]*Pharmacy Department of Guangxi Minzu Hospital, Nanning 530001, China*
[c]*Department of Pharmacology, Zhongshan School of Medicine, Sun Yat-sen University, Guangzhou 510080, China*

Abstract In this work, retinal penetration of fluorescein was achieved *in vitro* by covalent attachment of taurine to fluorescein, yielding the F–Tau conjugate. Nuclear magnetic resonance (NMR) and high resolution mass spectrometry (HRMS) were used to confirm the successful synthesis of F–Tau. The cellular uptake of F–Tau in adult retinal pigment epithelial cells (ARPE-19) and human retinal microvascular endothelial cells (hRMECs) was visualized *via* confocal scanning microscopy. The results indicated an improvement of solubility and a reduction of log$P$ of F–Tau compared with fluorescein. As compared with fluorescein, F–Tau showed little toxicity, and was retained longer by cells in uptake experiments. F–Tau also displayed higher transepithelial permeabilities than fluorescein in ARPE-19 and hRMECs monolayer cells ($P < 0.05$). These results showed that taurine may be a useful ligand for targeting small-molecule hydrophobic pharmaceuticals into the retina.

1. Introduction

Retinal diseases, such as retinal neuronal injury, age-related macular degeneration and cytomegalovirus retinitis, are important causes of blindness; yet the present medications for the treatment of retinal diseases are not ideal[1,2]. Topically-applied medications (drops) do not achieve the effective drug concentration in the retina due to the presence of corneal barriers. Local (e.g., intravitreal) injections are invasive, and can result in retinal detachment and endophthalmitis after repeated injections[3,4]. Although the extensive vascularization of the posterior of the eye might seem to predict favorable retinal penetration of systemically-administered drugs, the existing blood–retinal barrier (BRB) limits drug diffusion from blood to the retina. Thus, better methods are needed to facilitate the penetratration of the BRB following systemic administration of drugs for retinal diseases.

The BRB is composed of two parts, each providing some barrier functions[5]. The outer barrier (oBRB) contains the retinal pigment epithelium (RPE) which is located between the choroid and the neural retina. Under normal circumstances, RPE cells are tightly arranged and closely connected to the outer layer of the neural retina, providing an effective barrier between the neural retina and peripheral tissues. Exogenous substances do not easily enter the retina by penetrating the oBRB except for nutrients needed to maintain normal physiological functions. Some nutrients are selectively transported into the retinal layers by the RPE cells[6]. The second component of the BRB, the inner barrier (iBRB), is formed by the tightly-arranged retinal microvascular endothelial cells (RMECs) located within the vascular lumen. The iBRB isolates the retinal tissue from blood, thereby maintaining the stability of the neural retina by restricting the entry of toxic molecules, plasma, and water into the retina[6,7]. These components of the BRB explain why exogenous drugs have difficulty in penetrating the retina following systemic administration.

Taurine, an endogenous β-aminosulfonic acid, is important for cardiovascular, skeletal muscle and retinal health. Although taurine can be biochemically synthesized from cysteine in the liver[8], this pathway is not sufficient, resulting in a need for dietary taurine. Children may suffer from visual dysfunction during dietary taurine deficiency; this may be reversed by taurine supplements[9]. Exogenous taurine was reported to be actively transported by a taurine transporter (TauT) into cells[10–12]. As for the retina, taurine can be considered as an essential component in the development and maintenance of retinal form and function. The occurrence of retinitis, retinal degeneration, diabetic retinopathy and vision loss are closely related to the deficiency of taurine[12–14].

The physiological significance of taurine in the retina may be emphasized by the high levels of retinal taurine. Heinamaki et al.[15] reported that taurine is the most abundant free amino acid in the retina (12 μmol/g retina ≈ 12 mmol/L in rats), accounting for more than 50% of the free amino acid content[11]. In addition, the taurine concentration in the retina is about 100-fold greater than that in the serum (100–300 μmol/L)[16]. Such high levels of taurine may suggest powerful mechanisms for its accumulation in the retina. However, the retina-targeting ability of taurine is still unknown; therefore it is meaningful to investigate whether the taurine can be used as a tool to improve penetration of the BRB by exogenous drugs following systemic administration.

Based on the hypothesis described above, we firstly synthesized a taurine-conjugated fluorescein (F–Tau) by covalently attaching taurine to fluorescein. We then investigated the BRB-penetrating ability of F–Tau in two assembled monolayers of adult retina pigment epithelial cells (ARPE-19) and human retinal microvascular endothelial cells (hRMECs), two cell lines expressing TauT[17,18]. These experiments have investigated the retina-targeting potential of taurine.

2. Materials and methods

2.1. Materials and cells

Taurine (purity 98%) was purchased from TCI (Shanghai, China). Other reagents and solvents (analytical grade) from Aladdin (Shanghai, China) were used without further purification unless otherwise indicated. Silica gel (GF254, 300–400 mesh) based thin-layer chromatography was used to monitor the processes of reactions. NMR spectra were measured on a Bruker Avance III 400 MHz spectrometer. Chemical shifts were recorded in parts per million (ppm) using tetramethylsilane as an internal standard in dimethyl sulfoxide-d_6 (DMSO-d_6). Electrospray ionization-mass spectrometry (ESI-MS) was used to acquire the mass spectra on a TSQ Quantum Access Max (Thermo Scientific, San Jose, CA, USA). High resolution mass spectra (HRMS) of F–Tau were recorded using an Agilent Accurate-Mass-Q-TOF MS 6520 system under positive ionization mode. High-performance liquid chromatography (HPLC, Agilent 1200, USA) was performed to determine the purity of the compounds described in this paper. The purity of F–Tau was found to be higher than 95%.

ARPE-19 were kindly donated by Zhongshan Ophthalmic Center of Sun Yat-Sen University and hRMECs were bought from Guangzhou Jennio Biotech Co., Ltd. The cells were respectively cultured in Dulbecco's Modified Eagle media: nutrient mixture F-12 (DMEM/F12) and roswell park memorial institute 1640 (RPMI 1640) (Invitrogen, Grand Island, NY, USA) containing 10% fetal bovine serum, 1% penicillin (50 IU/mL) and streptomycin (50 μg/mL) in an atmosphere of 5% CO_2 at 37 °C.

2.2. Chemistry

2.2.1. The synthesis of the intermediate active ester (3)
Fluorescein 1 (3.32 g, 10 mmol), N-hydroxysuccinimide 2 (1.17 g, 10 mmol) and dicyclohexylcarbodiimide (DCC, 2.10 g, 10 mmol) in anhydrous dimethylformamide (DMF) were heated to 75 °C under nitrogen for 1.5 h. The resulting dicyclohexylurea (DCU) was filtered off at 0 °C and the solvent was evaporated under rotary evaporator at reduced pressure[19]. Then the crude residue was purified by silica column (Petroleum ether/Acetone, 3:1-1:1, v/v) to afford active ester 3 as red-orange solid, yielding 1.29 g (30%). ^{1}H NMR (400 MHz, DMSO-d_6): δ 11.07(s, 1H), 8.36(d, J = 8 Hz, 1H), 8.03(t, J = 4 Hz, 1 H), 7.90(t, J = 4 Hz, 1 H), 7.66(d, J = 8 Hz, 1H), 6.99–6.23(m, 6H), 2.72(s, 4H). MS (ESI): m/z 428.1 [M–H]$^-$ (Supplementary Figs. 1 and 2).

2.2.2. The synthesis of F–Tau (5)
The active ester 3 (1.00 g, 2.33 mmol) was dissolved in anhydrous DMF, to which taurine 4 (0.58 g, 4.66 mmol) and 0.65 mL of triethylamine (Et$_3$N, 4.66 mmol) that previously dried out under molecular screen cleaner were added. The obtained mixture was stirred at room temperature (RT) for 36 h and evaporated under rotary evaporator connected to a high vacuum. The crude residue was sequentially purified by silica column (ethyl acetate/ methanol, 4:1, v/v), ODS (octadecyl silane) column chromatography (methanol/H$_2$O) and preparative HPLC (acetonitrile/formic acid buffer) to afford the desired product F–Tau (5) as white powder, yielding 0.42 g (41%). ^{1}H NMR (400 MHz, DMSO-d_6):δ 8.34(br, 1 H), 7.79(dd, J = 4 Hz, 1H), 7.49(m, 2H), 6.98(dd, J = 4 Hz, 1H),

6.61(d, $J = 4$ Hz, 2H), 6.46(dd, $J = 8$ Hz, 2H), 6.39(d, $J = 8$ Hz, 2H), 3.26(t, $J = 8$ Hz, 2H), 2.17(t, $J = 8$ Hz, 2H); ^{13}C NMR (101 MHz, DMSO-d_6): δ166.71, 158.43 (2C), 153.30, 151.90 (2C), 132.56, 129.98, 128.56 (2C), 128.42, 123.51, 122.49, 112.07 (2C), 109.32 (2C), 102.39 (2C), 63.37, 49.18, 36.71; HRMS (ESI-TOF$^+$): m/z calcd. for $C_{22}H_{17}NO_7S$: 440.0798; found: 440.0796 [M+H]$^+$ (Supplementary Figs. 3–5).

2.3. Solubility studies

Saturated fluorescein and F–Tau solutions were obtained by dissolving excess fluorescein and F–Tau in doubly distilled water (2 mL) in centrifugal tubes respectively. Then the centrifugal tubes were shaken at 100 times/min at 25 °C for 24 h. After further still standing for 24 h at 25 °C, the saturated solutions were centrifuged and 20 μL of supernatant was injected into HPLC as described below (Section 2.7.4).

2.4. Estimation of logP

To determine the *n*-octanol/water partition coefficients of fluorescein and F–Tau, the traditional saturation shake flask methods were performed. After 24 h shaking of a conical flask containing *n*-octanol (30 mL) and double-distilled water (30 mL) at 100 times/min, *n*-octanol-saturated water and water-saturated *n*-octanol were obtained by centrifugation of the mixture at 4000 rpm for 10 min. Subsequently, fluorescein and F–Tau were dissolved in water-saturated *n*-octanol (2 mL), respectively. After adding 2 mL of *n*-octanol-saturated water, the mixture was shaken at 100 times/min at 25 °C for 24 h, centrifuged at 4000 rpm for 10 min and separated to obtain aqueous phases and oil phases. After proper dilution, 20 μL of aqueous phases or oil phases were injected into HPLC as described below (Section 2.7.4).

The partition coefficients (P) were calculated using the following equation:

$$P = C_0 / C_w \tag{1}$$

where C_0 means the drug concentration of oil phases and C_w represents the drug concentration of water phases.

2.5. MTT cytotoxicity assay

The cytotoxicities of fluorescein and F–Tau were assayed on ARPE-19 and hRMECs using the (3,4,5-dimethylthiazol-yl)-2,5-diphenyl-tetrazolium (MTT) assay. Briefly, ARPE-19 and hRMECs were seeded in 96-well plates at a density of 1×10^5 cells/well and cultured for 24 h at 37 °C. Then the cells were treated with different concentrations of fluorescein and F–Tau for 24 h followed by incubation with MTT (10 μL) (5.0 mg/μL, Sigma-Aldrich, St. Louis, MO, USA) for 4 h at 37 °C. Finally, the medium was replaced with 100 μL dimethyl sulfoxide (DMSO), and the optical density (OD) was determined with a microplate reader at a wavelength of 490 nm in triplicate. The cells viability was calculated using the following equation:

$$\text{Cells viability (\%)} = A_{490 \text{ nm Treated cells}} / A_{490 \text{ nm Control cells}} \times 100 \tag{2}$$

2.6. Cellular internalization

ARPE-19 and hRMECs, both expressing taurine transporter, were used for the cell internalization study. ARPE-19 and hRMECs were individually seeded on confocal dishes at a density of 5×10^3 cells/well and incubated for 24 h at 37 °C; then 100 μmol/L fluorescein and 100 μmol/L F–Tau were added to these cells and co-incubated for another 2 h and 6 h. The cells were washed for three times with Hank's balanced salt solution (HBSS, Ji Nuo Biology Co., Guangxi, China.) and the a Zeiss LSM 710 laser scanning confocal microscope (Carl Zeiss Meditec AG, Jena, Germany) was used to investigate the intracellular uptake (excitation wavelength for fluorescein: 488 nm, excitation wavelength for F–Tau: 405 nm).

2.7. Transport studies of fluorescein and F–Tau across monolayer cells in vitro

2.7.1. Transport studies of fluorescein and F–Tau across ARPE-19 monolayer cells[20,21]

Transport studies of fluorescein and F–Tau to pass through ARPE-19 monolayer cells were performed on 12-well plates containing Transwell® inserts with 0.4 μm pore size polycarbonate membrane (Corning Costar, Corning, NY, USA). Briefly, ARPE-19 were trypsinized, resuspended and seeded in the upper chamber at a density of 2.5×10^5 cells/well in 0.5 mL medium as well as 1.5 mL blank medium added in the lower chamber. Then the culture medium was replaced [0.5 mL in the apical (AP) side and 1.5 mL in the basolateral (BL) side] every other day for the first week and everyday after the first week. And when the transepithelial electrical resistance (TEER, Evom Epithelial Volt-ohm-meter, Sarasota, FL, USA) of the monolayer cells reached 150 Ω, the monolayer cells were employed in the transport studies[22,23].

Before transport experiments, the culture medium was removed and the monolayer cells were rinsed twice with preheated HBSS solution. Right before ARPE-19 transport studies, 0.5 mL pre-heated (37 °C) HBSS solution containing 100 μmol/L fluorescein or 100 μmol/L F–Tau was added to the AP side, while 1.5 mL preheated (37 °C) blank HBSS solution was loaded in the BL side. And then these plates were put in the atmosphere in 5% CO_2/ 37 °C. At indicated time intervals (30, 60, 120, 240 and 360 min), 100 μL of samples were taken from the receiver sides and immediately replaced with 100 μL fresh preheated blank HBSS solution. The TEER values of the monolayer maintained at about 150 Ω in the above processes. Those obtained samples were determined by HPLC as mentioned below (Section 2.7.4).

Apparent permeability coefficients (P_{app}) values were calculated using the equation:

$$P_{app} = (\Delta Q / \Delta t) / (A \times C_0) \tag{3}$$

where $\Delta Q / \Delta t$ is the linear appearance rate of mass in BP side, A is the filter/cell surface area (1.12 cm^2 for 12-well and 0.33 cm^2 for 24-well), and C_0 is the initial concentration of the test compounds.

2.7.2. Transport studies of fluorescein and F–Tau across hRMECs monolayer cells

Transport studies of fluorescein and F–Tau in hRMECs monolayer cells were performed on 24-well plates containing Transwell® inserts with 0.4 μm pore size polycarbonate membrane (Corning Costar, Corning, NY, USA). The general procedure for the transport studies of fluorescein and F–Tau across hRMECs monolayer cells was similar to that of ARPE-19 except the supplied medium was 0.15 mL to the AP side and 0.6 mL to the BP side. And the transport studies could be initiated when the TEER reached 200 Ω[24,25].
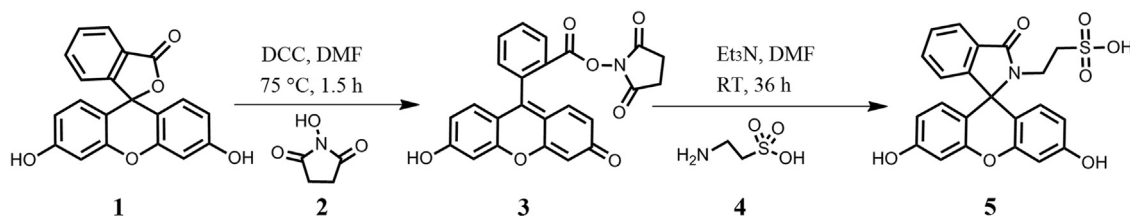
Scheme 1 Synthesis of F–Tau.
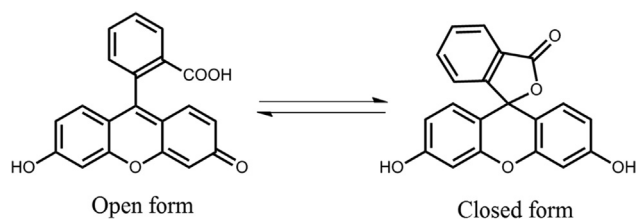
Scheme 2 The interconversion of fluorescein.

Table 1 Solubility and log$P$ of fluorescein and F–Tau.

Sample	Solubility (μg/mL)	log P
Fluorescein	6.75	1.55
F–Tau	10,852.54	− 1.03

Similarly, before the transport experiments, the culture medium in Transwell® inserts was removed and rinsed twice. And in hRMECs transport studies, preheated HBSS solution containing fluorescein or F–Tau (100 μmol/L, 0.15 mL) was added to the AP side while 0.6 mL of preheated blank HBSS solution loaded in the BL side. Also, at indicated time intervals (30, 60, 120, 240 and 360 min), 60 μL of samples were taken from the receiver sides and immediately replaced with 60 μL fresh preheated blank HBSS solution. The TEER values of the monolayer were still about 200 Ω in the above processes. Those obtained samples were determined by HPLC as mentioned below (Section 2.7.4).

2.7.3. Competition assay of transport studies

Free taurine was used as a competitive inhibitor to study whether the transportation of F–Tau was mediated *via* the TauT. ARPE-19 and hRMECs monolayer cells were prepared as described above. Before the transport studies, preheated HBSS solution containing taurine (10 mmol/L) was added to both the upper and lower chambers and incubated for 24 h in 5% CO_2 at 37 °C. Then the competitive transport experiments of the two monolayer cells proceeded as the transport studies described above. Those obtained samples were also determined by HPLC as mentioned below (Section 2.7.4).

2.7.4. HPLC analysis

The concentrations of fluorescein and F–Tau in the samples were analyzed by HPLC (Agilent 1200, USA) with Phenomenex Synergi Polar-RP (250 mm × 4.6 mm, 4 μm) at 35 °C. The ultraviolet detecting wavelength was set at 230 nm, and the injection volume was 20 μL. The mobile phase, consisting of phosphate buffer solution at pH 2.5 (phase A) and acetonitrile (phase B), was
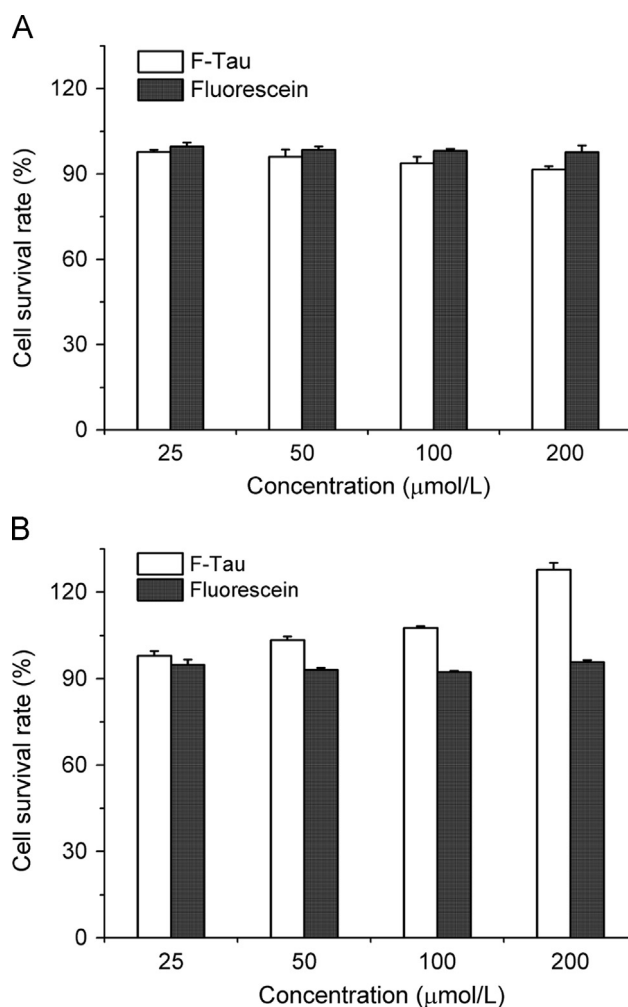

Figure 1 The survival rate (%) of hRMECs (A) and ARPE-19 (B) after incubated with fluorescein and F–Tau at various concentrations for 24 h ($n=6$). Data are presented as mean ± SD.

delivered at a flow rate of 1.0 mL/min. The isocratic elution method (50:50, *v/v*) was used to analyze fluorescein in 12 min. And the gradient elution method was used to analyze F–Tau by varing the percentages of phase A and phase B from 70:30 to 58:42 in 15 min.

2.8. Data analysis

Data were expressed as means ± standard deviation (SD). Statistical significance of the difference was assessed by one-way analysis of variance to determine the significance among groups

in SPSS 19.0 software (IBM Corporation, Armonk, NY, USA). A *P* value <0.05 was considered significant.

3. Results and discussion

3.1. Synthetic routes

The synthetic pathway for F–Tau is illustrated in Scheme 1. Traditionally, fluorescein has been viewed to exist in two forms (Scheme 2): a highly fluorescent, open, quinone form and a non-fluorescent, closed, spirolactone form[26]. In order to obtain F–Tau, the first step involved the activation of fluorescein because it was difficult to react with primary amines like taurine when the carboxyl group was masked. After fluorescein was activated to the open form by reacting with *N*-hydroxysuccinimide (which has a good leaving group), taurine could react rapidly with this active ester in DMF under alkaline condition at ambient temperature. Surprisingly, we found the intensely red-orange active ester solution was converted into a nearly colorless solution after the reaction and the non-fluorescent white solid (F–Tau) was isolated by preparative HPLC. The resulting F–Tau was in a closed, spiro-lactam form, consistent with the results of Adamczyk and Grote[26]. This configuration was confirmed by the characteristic spirolactam peak near 64 ppm in the ^{13}C NMR spectrum (Supplementary Fig. 4)[26]. After intravenous injection, this closed-spirolactam form of F–Tau was expected to be opened by lactamase, resulting in an open form of taurine conjugate exposing the effective structure of taurine. The newly-formed taurine conjugate would then be specifically recognized and actively transported by the taurine transporter, resulting is penetration of the BRB.

3.2. Physicochemical properties of F–Tau

As shown in Table 1, the solubility of F–Tau increased nearly 1600-fold compared with fluorescein due to the presence of polar sulfonic acid group. The latter facilitates F–Tau's initial water solubility. In addition, the partition coefficient of F–Tau was sharply reduced as compared with that of fluorescein, decreasing from the original 1.55 to −1.03 (Table 1). As compared with highly lipophilic drugs, this reduction in log *P* value might be beneficial in reducing drug efflux from the cells, thereby extending residence time in the cell. Above all, the introduction of taurine might enhance the exposure dose and exposure time of fluorescein *in vivo*, thereby improving the efficacy of the drug.

3.3. Cytotoxicity

To screen the appropriate concentration of F–Tau for transport experiments on ARPE-19 and hRMECs monolayer cells, the survival rates of the two cells exposed to various concentrations of F–Tau were measured by the MTT assay (Fig. 1). At dose levels of 0–200 μmol/L F–Tau showed no toxicity on hRMECs (Fig. 1A) and even exhibited a slight promotion of growth for ARPE-19 (Fig. 1B). Thus, taurine can be safely used as a ligand in these studies. Incorporating the limit of detection of the HPLC and the condition of cells into account, a concentration of 100 μmol/L F–Tau and fluorescein was used in the following studies.

3.4. Cellular uptake assay

As shown in Fig. 2, strong fluorescence was observed in ARPE-19 (AF2 and AT2) and hRMECs (hF2 and hT2) after treatment with
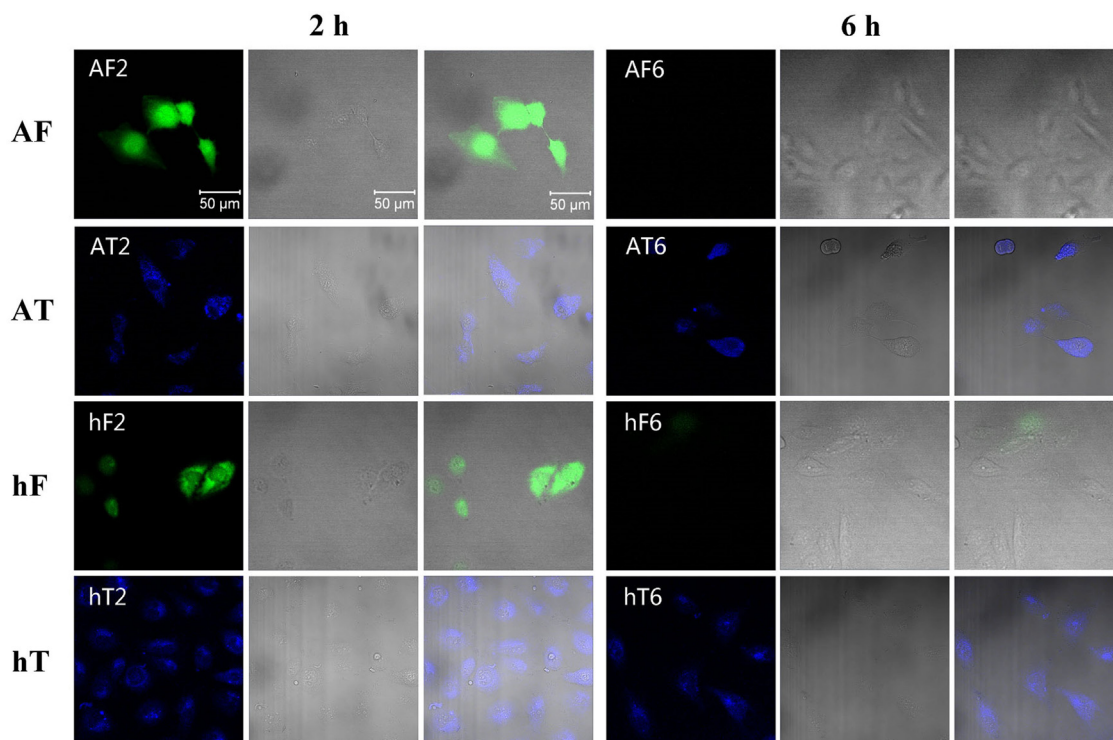

Figure 2 Confocal scanning microscopy images of APRE-19 (A) and hRMECs cells (h) incubated with free fluorescein (AF and hF) and free F–Tau (AT and hT). The number on the right side of the alphabet was represented for the incubated time at 37 °C. Green: fluorescence of fluorescein. Blue: fluorescence of F–Tau.
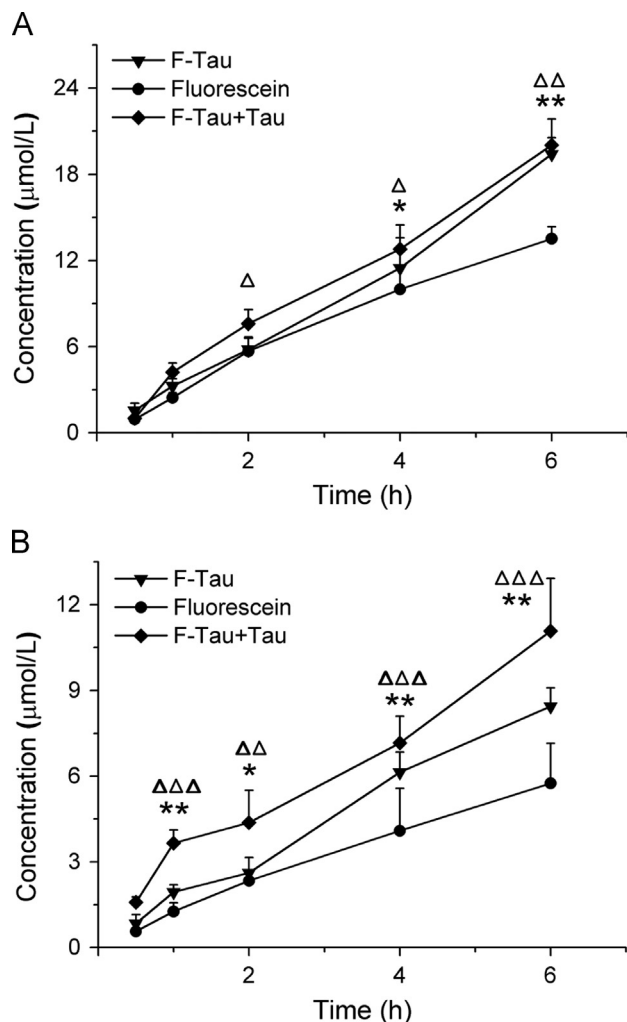
Figure 3   The time profiles of transport experiment across ARPE-19 (A) and hRMECs (B) monolayer ($n=3$). *$P<0.05$, **$P<0.01$, *F–Tau *versus* fluorescein. $^{\triangle}P<0.05$, $^{\triangle\triangle}P<0.01$, $^{\triangle\triangle\triangle}P<0.001$, $^{\triangle}$F–Tau+Tau *versus* fluorescein.

Table 2   Effect of taurine on P_{app} values of F–Tau across ARPE-19 and hRMECs monolayer cells.

Test drug	P_{app} ($\times 10^6$ cm/s)		Ratio($P_{app, \text{Test Drug-to-Fluoresein}}$)	
	ARPE-19	hRMECs	ARPE-19	hRMECs
Tau	7.72 ± 1.13	10.67 ± 0.36	1.39	1.47
F–Tau+Tau	7.79 ± 1.01	13.30 ± 0.91	1.40	1.84
Fluorescein	5.56 ± 0.80	7.23 ± 0.92	–	–

Tau is presented as taurine. P_{app} values are presented as mean$\pm$SD ($n=3$).

F–Tau and fluorescein for 2 h at 37 °C. This suggested that both fluorescein and F–Tau could be internalized by the two kinds of cells. Interestingly, after 6 h incubation, almost no fluorescein was observed in the fluorescein groups (AF6 and hF6), whereas fluorescence was still seen in the F–Tau groups (AT6 and hT6) in both cell lines. The high lipophilicity of fluorescein may make it easy to be internalized by the cells within 2 h at first and be inclined to be excluded during the next 4 h by the same reason. Meanwhile the lower log P value of F–Tau was thought to reduce the probability of efflux, yielding weak fluorescence 6 h after incubation. These results showed that incorporation of taurine extends the retention time of fluorescein in the retina cells.

3.5. Transportation of fluorescein and F–Tau across the monolayer cells in vitro

To determine the transepithelial permeability of fluorescein and F–Tau, the transport studies were carried out on ARPE-19 (Fig. 3A) and hRMECs (Fig. 3B) monolayer cells in transwell® inserts. The two monolayer cells were established to serve as the permeability barriers for BRB according to the permeability coefficients[20]. The relatively apparent permeability ratio was obtained by the equation:

$$\text{Ratio}(P_{app, \text{A to B}}) = P_{app, \text{A}}/P_{app, \text{B.}} \tag{4}$$

where Ratio ($P_{app,\text{A to B}}$) represents the relatively apparent permeability ratio of drug A and drug B, $P_{app, \text{A}}$ and $P_{app, \text{B}}$, respectively, represent the apparent permeability coefficients of drug A and drug B. Table 2 summarized the permeability values of F–Tau and fluorescein across ARPE-19 and hRMECs monolayer cells. The permeability of F–Tau across the two monolayer cells was both higher than that of fluorescein, 7.72 *versus* 5.56 on ARPE-19 and 10.67 *versus* 7.23 on hRMECs, and the Ratio ($P_{app, \text{F–Tau to fluorescein}}$) was up to 1.39 and 1.47, respectively. These results suggested that F–Tau, the conjugate of fluorescein by conjugating taurine to fluorescein, notably elevated the cell barrier penetration of fluorescein.

Several possible explanations for the increased penetration of F–Tau can be considered. Firstly, molecular size cannot explain these results because the molecular volume of fluorescein is smaller than that of F–Tau. Secondly, membrane solubility is not a factor because fluorescein is more lipid soluble than F–Tau. Furthermore, F–Tau and fluorescein could be seen to internalize to the interior cell in the uptake experiments, suggesting that the penetrating characteristics of F–Tau are relevant. Considering the contradictory phenomena of low log P value and the high penetration of F–Tau, we may reasonably conclude that the transport of F–Tau is mediated *via* a specific transporter, and that this transporter may improve the penetrability of fluorescein to retinal cells.

3.6. Transport mechanisms of fluorescein and F–Tau across monolayers in vitro

After pre-incubation with 10 mmol/L taurine, F–Tau accumulation was significant ($P<0.05$), similar to that seen without pre-incubation; Ratios ($P_{app, \text{F–Tau+Tau to fluorescein}}$) of 1.40 and 1.84 were observed on ARPE-19 and hRMECs monolayers. But as shown in Fig. 3 and Table 2, the transport of F–Tau in cells previously incubated with free taurine did not show the inhibition, but rather an increase in the pentration of ARPE-19 and hRMECs monolayer cells; the resulting $P_{app, \text{F–Tau+Tau to F–Tau}}$ values ranged from 7.79 to 7.72 on ARPE-19 and 13.30 to 10.67 on hRMECs. One possible answer for these unexpected results was that free taurine, used as the competitive inhibitor, may have activated other transport pathways to improve the penetrability of F–Tau as

reported in other studies[27,28]. Identification of such transporters requires further studies[29].

4. Conclusions

There is an urgent need for the development of improved treatments for many retina diseases. The BRB significantly impedes the delivery of many systemically-administered medications for treating the retina. In this study, we investigated an effective retina-targeting ligand to increase the BRB permeability of drugs. Since exogenous taurine is concentrated in the retina where it functions as a neuroprotective agent, this compound was chosen to evaluate its retina-targeting efficacy. F–Tau, synthesized by conjugating taurine to fluorescein, was studied for this purpose. The results indicated that the introduction of taurine could result in an improvement of solubility, a reduction of log P and a prolonged residence time of F–Tau on the cells compared with fluorescein. The transport studies also indicated that the introduction of taurine exhibited significantly strong transepithelial permeability across the retinal cell barriers *in vitro*. Taurine may be a promising ligand for the delivery of retina-targeted medications.

Appendix A. Supplementary material

Supplementary data associated with this article can be found in the online version at http://dx.doi.org/10.1016/j.apsb.2014.10.006.

References

1. Del Amo EM, Urtti A. Current and future ophthalmic drug delivery systems. A shift to the posterior segment. *Drug Discov Today* 2008;**13**:135–43.
2. Hughes PM, Olejnik O, Chang-Lin JE, Wilson CG. Topical and systemic drug delivery to the posterior segments. *Adv Drug Deliv Rev* 2005;**57**:2010–32.
3. Bochot A, Couvreur P, Fattal E. Intravitreal administration of antisense oligonucleotides: potential of liposomal delivery. *Prog Retin Eye Res* 2000;**19**:131–47.
4. Ausayakhun S, Yuvaves P, Ngamtiphakom S, Prasitsilp J. Treatment of cytomegalovirus retinitis in AIDS patients with intravitreal ganciclovir. *J Med Assoc Thai* 2005;**88 Suppl 9**:S15–20.
5. Campbell M, Humphries P. The blood–retina barrier: tight junctions and barrier modulation. *Adv Exp Med Biol* 2012;**763**:70–84.
6. Duvvuri S, Majumdar S, Mitra AK. Drug delivery to the retina: challenges and opportunities. *Expert Opin Biol Ther* 2003;**3**:45–56.
7. Cunha-Vaz JG. The blood-ocular barriers: past, present, and future. *Doc Ophthalmol* 1997;**93**:149–57.
8. Hansen SH. The role of taurine in diabetes and the development of diabetic complications. *Diabetes Metab Res Rev* 2001;**17**:330–46.
9. Geggel HS, Ament ME, Heckenlively JR, Martin DA, Kopple JD. Nutritional requirement for taurine in patients receiving long-term parenteral nutrition. *New Engl J Med* 1985;**312**:142–6.
10. Yahara T, Tachikawa M, Akanuma S, Kubo Y, Hosoya K. Amino acid residues involved in the substrate specificity of TauT/SLC6A6 for taurine and gamma-aminobutyric acid. *Biol Pharm Bull* 2014;**37**:817–825.
11. Spaeth DG, Schneider DL, Sarett HP. Taurine synthesis, concentration, and bile salt conjugation in rat, guinea pig, and rabbit. *Proc Soc Exp Biol Med* 1974;**147**:855–8.
12. Heller-Stilb B, Van RC, Rascher K, Rascher K, Hartwiq HG, Huth A, et al. Disruption of the taurine transporter gene (taut) leads to retinal degeneration in mice. *FASEB J* 2002;**16**:231–3.
13. Militante J, Lombardini JB. Age-related retinal degeneration in animal models of aging: possible involvement of taurine deficiency and oxidative stress. *Neurochem Res* 2004;**29**:151–60.
14. De Luca G, Calpona PR, Caponetti A, Romano G, Di Benedetto A, Cucinotta D, et al. Taurine and osmoregulation: platelet taurine content, uptake, and release in type 2 diabetic patients. *Metabolism* 2001;**50**:60–4.
15. Heinamaki AA, Muhonen AS, Piha RS. Taurine and other free amino acids in the retina, vitreous, lens, iris-ciliary body, and cornea of the rat eye. *Neurochem Res* 1986;**11**:535–42.
16. Tornquist P, Alm A. Carrier-mediated transport of amino acids through the blood–retinal and the blood–brain barriers. *Graefes Arch Clin Exp Ophthalmol* 1986;**224**:21–5.
17. Tomi M, Terayama T, Isobe T, Egami F, Morito A, Kurachi M, et al. Function and regulation of taurine transport at the inner blood-retinal barrier. *Microvasc Res* 2007;**73**:100–6.
18. Bridges CC, Ola MS, Prasad PD, El-Sherbeny A, Ganapathy V, Smith SB. Regulation of taurine transporter expression by NO in cultured human retinal pigment epithelial cells. *Am J Physiol Cell Physiol* 2001;**281**:C1825–36.
19. Gao J, Wang P, Giese RW. Xanthamide fluorescent dyes. *Anal Chem* 2002;**74**:6397–401.
20. Tang F, Ouyang H, Yang JZ, Borchardt RT. Bidirectional transport of rhodamine 123 and Hoechst 33342, fluorescence probes of the binding sites on P-glycoprotein, across MDCK-MDR1 cell monolayers. *J Pharm Sci* 2004;**93**:1185–94.
21. Li L, Tuo J, Xie YQ, Huang MH, Huang M, Pi RB, et al. Preparation, transportation mechanisms and brain-targeting evaluation *in vivo* of a chemical delivery system exploiting the blood–cerebrospinal fluid barrier. *J Drug Target* 2014;**22**:724–31.
22. Hornof M, Toropainen E, Urtti A. Cell culture models of the ocular barriers. *Eur J Pharm Biopharm* 2005;**60**:207–25.
23. Barar J, Asadi M, Mortazavi-Tabatabaei SA, Omidi Y. Ocular drug delivery; impact of *in vitro* cell culture models. *J Ophthalmic Vis Res* 2009;**4**:238–52.
24. Gillies MC, Su T, Naidoo D. Electrical resistance and macromolecular permeability of retinal capillary endothelial cells *in vitro*. *Curr Eye Res* 1995;**14**:435–42.
25. Tretiach M, van Driel D, Gillies MC. Transendothelial electrical resistance of bovine retinal capillary endothelial cells is influenced by cell growth patterns: an ultrastructural study. *Clin Exp Ophthalmol* 2003;**31**:348–53.
26. Adamczyk M, Grote J. Efficient fluorescein spirolactam and bis-spirolactam synthesis. *Synth Commun* 2001;**17**:2681–90.
27. Huang H, Dao DW, Qin LH, Tian SQ, Liang Y, Pan SR, et al. Dilution-stable PAMAM G1-grafted polyrotaxane supermolecules deliver gene into cells through a caveolae-dependent pathway. *Mol Pharm* 2014;**11**:2323–33.
28. Perumal OP, Inapagolla R, Kannan S, Kannan RM. The effect of surface functionality on cellular trafficking of dendrimers. *Biomaterials* 2008;**29**:3469–76.
29. Anderson CM, Howard A, Walters JR, Ganapathy V, Thwaites DT. Taurine uptake across the human intestinal brush-border membrane is *via* two transporters: H$^+$-coupled PAT1 (SLC36A1) and Na$^+$- and Cl$^-$-dependent TauT (SLC6A6). *J Physiol* 2009;**587**:731–44.